This is an open access article published under an ACS AuthorChoice License, which permits copying and redistribution of the article or any adaptations for non-commercial purposes.

BIOCHEMISTRY
including biophysical chemistry & molecular biology

Article

pubs.acs.org/biochemistry

Entamoeba histolytica RacC Selectively Engages p21-Activated Kinase Effectors

Dustin E. Bosch[†] and David P. Siderovski*[,‡]

[†]Department of Pharmacology, The University of North Carolina, Chapel Hill, North Carolina 27514, United States

[‡]Department of Physiology & Pharmacology, West Virginia University School of Medicine, Robert C. Byrd Health Sciences Center, Morgantown, West Virginia 26506, United States

Supporting Information

ABSTRACT: Rho family GTPases modulate actin cytoskeleton dynamics by signaling through multiple effectors, including the p21-activated kinases (PAKs). The intestinal parasite *Entamoeba histolytica* expresses ~20 Rho family GTPases and seven isoforms of PAK, two of which have been implicated in pathogenesis-related processes such as amoebic motility and invasion and host cell phagocytosis. Here, we describe two previously unstudied PAK isoforms, EhPAK4 and EhPAK5, as highly specific effectors of EhRacC. A structural model based on 2.35 Å X-ray crystallographic data of a complex between EhRacC^{Q65L}·GTP and the EhPAK4 p21 binding domain (PBD) reveals a fairly well-conserved Rho/effector interface despite deviation of the PBD α-helix. A structural comparison with EhRho1 in complex with EhFormin1 suggests likely determinants of Rho family GTPase signaling specificity in *E. histolytica*. These findings suggest a high degree of Rho family GTPase diversity and specificity in the single-cell parasite *E. histolytica*. Because PAKs regulate pathogenesis-related processes in *E. histolytica*, they may be valid pharmacologic targets for anti-amoebiasis drugs.

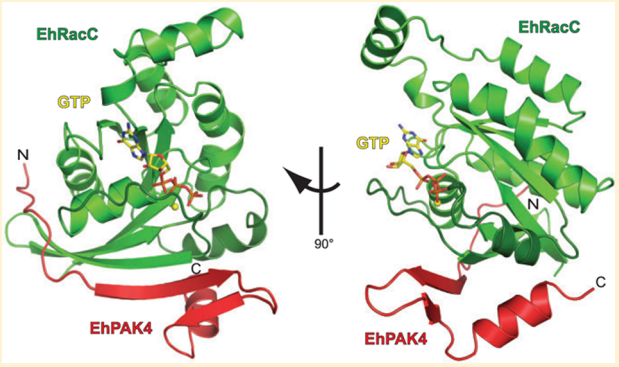

Rho family GTPases are master regulators of multiple key cellular processes such as cell division, transcription, and, most prominently, dynamic reorganization of the actin cytoskeleton.[1,2] Inactive, GDP-bound Rho GTPases are activated by guanine nucleotide exchange factors (GEFs) that promote release of GDP and subsequent binding of GTP.[3,4] Rho GTPases undergo a conformational change dominated by two mobile switch regions upon binding GTP, allowing engagement of downstream effectors.[2] Among the established Rho family GTPase effectors are the p21-activated kinases, or PAKs, that contain an N-terminal regulatory domain with a p21 binding domain (PBD) and a C-terminal kinase domain.[5] The six mammalian PAKs can be classified into two groups with distinct structural features and mechanisms of activation.[6] The regulatory domains of group I PAKs (PAK1−3) contain an autoinhibitory domain (AID) that partially overlaps with the PBD.[5] The C-terminal portion of the AID, termed the kinase inhibitory domain (KI), lies in the catalytic cleft of the kinase domain, preventing efficient phosphorylation of PAK substrates in the absence of active Rho GTPase.[7] Activation of the best-studied group member, PAK1, occurs through a multistep process involving binding of Cdc42 or Rac to the PBD, reorganization of the KI, and phosphorylation of the kinase domain activation loop.[7] Once activated, PAK1 phosphorylates numerous signaling proteins, including β-catenin and the mitogen-activated protein kinase kinase MEK1.[8,9] In contrast, early studies of group II PAKs detected higher basal levels of kinase activity that were not dramatically altered upon interaction with Cdc42 or Rac, suggesting Rho family GTPase-dependent localization of PAK, rather than auto-inhibition, as the primary mode of group II PAK signaling.[5] More recent studies suggest the presence of a structurally distinct but functionally similar autoinhibitory segment in group II PAKs.[6] Although activation loop phosphorylation is constitutive, binding of Cdc42 or Rac to the PBD is thought to be required to displace the autoinhibitory segment and promote full activation of group II PAKs.[6] Human PAKs have emerged as drug targets, particularly in specific cancers.[10,11] For instance, the small molecule IPA-3 was recently identified as a covalent modifier and inhibitor of PAK1 activation.[12,13]

The intestinal parasite *Entamoeba histolytica* is the causative agent of amoebic colitis and systemic amoebiasis.[14] Encysted *E. histolytica* is spread primarily through contaminated food and water sources among poor populations of developing countries, although outbreaks among travelers and susceptible populations occur in the United States.[14] *E. histolytica* cysts cycle to the trophozoite form in the human intestine and may give rise

Received: September 29, 2014
Revised: December 21, 2014
Published: December 22, 2014

 © 2014 American Chemical Society

DOI: 10.1021/bi501226f
Biochemistry 2015, 54, 404−412

to local destruction of the intestinal mucosa (amoebic colitis) or more rarely may enter the bloodstream, leading to systemic amoebiasis characterized by liver, lung, and brain abscesses.[15] The pathogenesis of *E. histolytica* infection depends on a highly dynamic, actin-rich trophozoite cytoskeleton.[16] Single-cell trophozoites express ~20 Rho family GTPases and downstream signaling effectors important for coordination of actin cytoskeletal rearrangement in pathogenesis-related processes, including migration and chemotaxis, adherence to intestinal epithelium, and host cell killing and phagocytosis (reviewed in ref 17). For instance, expression of constitutively active EhRacA or EhRacG in *E. histolytica* trophozoites alters phagocytosis and surface receptor capping,[18,19] while EhRho1 engages a diaphanous-related formin effector, EhFormin1, to directly modulate actin polymerization.[20,21] EhRacC directly interacts with the heterotrimeric G protein effector EhRGS-RhoGEF and, together with EhGα1, promotes Rac GTPase activation in cells.[22]

Six PBD-containing kinases related to mammalian PAKs are also encoded by the *E. histolytica* genome.[17,23] An additional protein, EhPAK (also called EhPAK1), does not contain a conserved PBD but was found to bind human Rac1 at its N-terminus.[24] EhPAK1 localizes to the leading edge of migrating trophozoites and is implicated in amoeboid migration, polarity, and human red blood cell phagocytosis.[24] EhPAK2 has a role in collagen matrix invasion, and its PBD selectively engages activated EhRacA.[17,23] A third studied PAK, EhPAK3, autophosphorylates *in vivo* and displays *in vitro* kinase activity in the absence of small GTPases.[25] Thus, *E. histolytica* PAKs regulate pathogenesis-related processes, particularly trophozoite migration and extracellular matrix invasion. However, the relationship of *E. histolytica* PAK isoforms to mammalian PAKs remains unclear; specifically, it is not known how their activation mechanisms are related to mammalian group I and group II modes of autoinhibition. The degree of Rho family GTPase/PAK signaling specificity in *E. histolytica* is also an unresolved question, given the apparent simultaneous expression of ~20 Rho family GTPases and up to seven PAKs in a single-cell organism. Here, we quantify the GTPase binding selectivity of two previously unstudied *E. histolytica* PAKs and determine the structural relationship of the EhRacC/EhPAK4 PBD interface to mammalian homologues.

EXPERIMENTAL PROCEDURES

Cloning and Protein Purification. Genomic DNA was isolated from the virulent HM-1:IMSS strain of *E. histolytica* using a DNeasy Blood and Tissue Kit (Qiagen). EhRho1, EhRacC, EhRacD, and EhRacG were cloned from genomic DNA by polymerase chain reaction (PCR) amplification as hexahistidine-tagged open reading frame fusions, expressed in B834 *Escherichia coli*, purified by nickel affinity and gel filtration chromatography, and loaded with nucleotide as described previously.[21] For EhRacC (AmoebaDB accession number EHI_070730) used in crystallographic experiments, the flexible C-terminal tail that includes the *CaaX* prenylation motif (11 residues) was excluded, and a glutamine (Q65) required for GTPase activity was mutated to leucine using the two-PCR method.[26] The EhRacC^{Q65L} N-terminal hexahistidine tag was removed with tobacco etch virus (TEV) prior to NTA affinity chromatography and gel filtration, as described previously for EhRho1.[20] Open reading frames of the isolated p21 binding domains (PBDs) of EhPAK4 (EHI_152540, amino acids 12−78) and EhPAK5 (EHI_043140, amino acids 105−161) were amplified via PCR from genomic DNA and subcloned as hexahistidine fusions into a pET vector-based ligation-independent cloning vector, pLIC-His, as described previously.[20] The following PCR primer sequences were used: EhPAK4, 5′-GAACTTATCATTTCTGATC-3′ and 5′-TTATGTTCTATTTCCATTATC-3′; and EhPAK5, 5′-GATATTAGTGAACCAACAG-3′ and 5′-TTATTGTGTGAATTCTAATAC-3′. For each *E. histolytica* PAK, B834 *Es. coli* cells were grown to an OD_{600} of 0.8 at 37 °C and expression was induced with 500 mM isopropyl β-D-thiogalactopyranoside (IPTG) for 14−16 h at 20 °C. Pelleted bacterial cells were resuspended in N1 buffer containing 30 mM HEPES (pH 8.0), 250 mM NaCl, and 30 mM imidazole and lysed by high-pressure homogenization with an Emulsiflex (Avestin, Ottawa, ON). Cellular lysates were cleared by centrifugation at 100000*g* for 1 h at 4 °C, and the supernatant was applied to a nickel-nitrilotriacetic acid (NTA) FPLC column (GE Healthcare), washed extensively with N1, and eluted in N1 buffer with 300 mM imidzaole. For proteins used in biochemical experiments, eluted protein was pooled and resolved using a size exclusion column (HiLoad 16/60 Superdex 200, GE Healthcare) in S200 buffer containing 50 mM HEPES (pH 7.5), 100 mM NaCl, and 5 mM DTT. For proteins used in crystallographic studies, protein eluted from the NTA column was pooled and dialyzed into imidazole-free N1 supplemented with 5 mM DTT overnight at 4 °C in the presence of His_6-tobacco etch virus (TEV) protease to cleave the N-terminal affinity tag. The dialysate was then passed over a second NTA column to remove TEV protease and uncleaved protein, followed by resolution by size exclusion in S200 buffer. Proteins were concentrated to 0.25−2 mM and snap-frozen in a dry ice/ethanol bath for storage at −80 °C. The protein concentration was determined by A_{280} measurements upon denaturation in 8 M guanidine hydrochloride, based on predicted extinction coefficients for each protein.

Crystallization and Determination of the Structure of the EhRacC^{Q65L}·GTP/EhPAK4 PBD Complex. A stable 1:1 complex of EhRacC^{Q65L}·GTP and EhPAK4 PBD was assembled over a gel filtration column. Crystals were obtained by vapor diffusion from hanging drops at 18 °C by mixing the EhRacC^{Q65L}·GTP/EhPAK4 complex (13 mg/mL) in a 1:1 ratio with a crystallization solution containing 22% (w/v) PEG 4000, 200 mM $MgCl_2$, and 100 mM MES (pH 6.5). Crystals grew to ~300 μm × 200 μm × 100 μm over 5−7 days, exhibiting the symmetry of space group $P2_1$ (a = 49.3 Å, b = 212.0 Å, c = 49.8 Å, $\alpha = \gamma = 90°$, and β = 102.8°) and containing four EhRacC^{Q65L}·GTP/EhPAK4 dimers in the asymmetric unit (Table 1). For the collection of data at 100 K, crystals were serially transferred for ~1 min into a crystallization solution supplemented with 30% (v/v) glycerol in 10% increments and plunged into liquid nitrogen. Native data sets were collected at the GM/CA-CAT 23-ID-B beamline at the Advanced Photon Source (Argonne National Laboratory, Argonne, IL). Data were processed using HKL2000.[27] A structural model of human Rac1 from X-ray crystallography [Protein Data Bank (PDB) entry 3TH5], modified to exclude bound nucleotide and magnesium, served as a molecular replacement search model using PHENIX AutoMR.[28] Upon molecular replacement, strong electron density was observed for GTP and magnesium, as well as the secondary structural elements of the EhPAK4 PBD. The EhPAK4 structural model was manually built with alternating iterations of refinement. Refinement was conducted using phenix.refine,[28] interspersed with manual revisions of the model using Coot.[29] Refinement consisted of conjugate

DOI: 10.1021/bi501226f
Biochemistry 2015, 54, 404−412

Table 1. Data Collection and Refinement Statistics for EhRacC^{Q65L}/EhPAK4 (PDB entry 4MIT)

Data Collection[a]	
space group	$P2_1$
cell dimensions	
a, *b*, *c* (Å)	49.32, 211.96, 49.78
α, β, γ (deg)	90.0, 102.85, 90
wavelength (Å)	1.000
resolution (Å)	46.9−2.35 (2.37−2.35)
no. of unique reflections	36818 (910)
R_{merge} (%)	6.7 (68.7)[b]
$I/\sigma I$	34.7 (2.2)
completeness (%)	87.0 (85.0)
redundancy	5.0 (5.3)
Wilson *B* factor (Å^2)	48.5
Refinement[a]	
resolution (Å)	46.9−2.35 (2.39−2.35)
no. of reflections	36744 (1754)
R_{work}/R_{free} (%)	17.6/22.0 (24.0/30.4)
no. of atoms	
protein	6874
ligand/ion	140
water	341
average *B* factor (Å^2)	
protein	36.2
ligand/ion	30.6
water	34.6
root-mean-square deviation	
bond lengths (Å)	0.013
bond angles (deg)	1.277

[a]Values in parentheses are for the highest-resolution shell. [b]All data were collected from a single crystal.

gradient minimization and calculation of individual anisotropic displacement and translation/libration/screw (TLS) parameters.[30] The current model contains four EhRacC^{Q65L}·GTP/EhPAK4 PBD dimers in the asymmetric unit. EhRacC residues 1−4 and 182 in chain A, residues 1−4 in chain B, residues 1 and 2 in chain C, and residues 1 and 2 in chain D could not be located in the electron density. EhPAK4 residues 52−78 in chain E, residues 1 and 51−78 in chain F, and residues 52−78 in chains G and H could not be located in the electron density. Ramachandran plot analysis indicated 98.5% favored, 1.5% allowed, and 0% disallowed residues.

Surface Plasmon Resonance (SPR) Assays. SPR-based measurements of protein−protein interactions were performed on a Biacore 3000 (GE Healthcare) and a Bio-Rad ProteOn XPR36 instrument, essentially as described previously.[20] Briefly, purified His$_6$-EhPAK4 PBD and His$_6$-EhPAK5 PBD proteins were separately immobilized on an NTA biosensor chip using covalent capture coupling.[31] EhRacC, EhRacC^{Q65L}, EhRacD, EhRacG, or EhRho1 was injected in 30−100 μL volumes at increasing concentrations. Experiments were performed in a running buffer containing 50 mM HEPES (pH 7.4), 150 mM NaCl, 0.05% NP-40 alternative (Calbiochem), 50 μM EDTA, and 1 mM $MgCl_2$. Background changes in refractive index upon injection of samples were subtracted from all curves using BIAevaluation version 3.0 (GE Healthcare) or ProteOn Manager (Bio-Rad). Equilibrium binding analyses were conducted as previously described[32] using GraphPad Prism version 5.0 to determine binding affinities. Kinetic analyses were performed on triplicate Rho GTPase injections as previously described.[33]

RESULTS

***E. histolytica* PAK Genes Resemble Mammalian Group I PAKs.** The *E. histolytica* genome encodes seven putative p21-activated kinases (PAKs),[34] three of which have been previously characterized.[23−25,35] Although three *E. histolytica* PAKs possess N-terminal PH domains not seen in mammalian PAKs,[23] the p21 binding domains (PBDs) in *E. histolytica* are significantly similar with those of mammalian PAKs (Figure 1). The protein sequences immediately C-terminal to the PBDs in all *E. histolytica* PAKs resemble the mammalian group I PAK autoinhibitory domains (AIDs), distinct from the group II PAKs (Figure 1B).[5] The average level of sequence identity of EhPAK4 was 52% compared to human group I PAKs and 37% compared to human group II PAKs (Figure S1 of the Supporting Information). Although this similarity of the AIDs suggests a shared evolutionary origin and possibly a shared autoinhibitory mechanism with mammalian group I PAKs, sequence similarity breaks sharply prior to the C-terminal portion of the AID, termed the kinase inhibitory domain (KI) (Figure 1B). In human PAK1, this segment is known to directly inhibit the kinase active site, with a particularly important role for Lys141.[7] The absence of a clear KI counterpart in the *E. histolytica* PAKs suggests either a lack of autoinhibition or an autoinhibitory mechanism different from that of mammalian homologues.

EhRacC Selectively Engages Two Putative PAK Effectors. To further investigate the signaling specificity among the ∼20 Rho family GTPases expressed in *E. histolytica* and their effectors, the PBDs from two previously uncharacterized PAKs, EhPAK4 and EhPAK5, were cloned from genomic DNA, expressed and purified from *Es. coli*, and immobilized for surface plasmon resonance binding experiments. Of four activated Rho GTPases tested, only a GTPase-deficient EhRacC mutant (Q65L) exhibited specific binding to both EhPAK4 and EhPAK5 (Figure 2). Equilibrium binding analyses revealed affinity constants (K_D) of 170 ± 30 nM and 1.9 ± 0.2 μM for EhPAK4 and EhPAK5 PBDs, respectively, as well as a high degree of nucleotide state selective binding to EhRacC, typical of Rho GTPase/effector interactions. Kinetic analyses of both EhRacC/PAK interactions using triplicate analyte injections indicated an ∼2.6-fold faster rate of EhRacC association (k_{on}) and an ∼3.3-fold slower rate of EhRacC dissociation (k_{off}) for EhPAK4 than for EhPAK5, consistent with an order of magnitude difference in binding affinity (Figure 2). The sequence diversity of the EhPAK PBDs, in contrast to the closely related human PAK PBDs, likely allows for interaction with a larger number of Rho family GTPases in *E. histolytica* (Figure 1B); e.g., EhPAK2 engages activated EhRacA,[23] while EhPAK4 and -5 each interact with activated EhRacC. In support of this hypothesis, sequence identities of *E. histolytica* and human PAK PBDs were calculated (Figure S1 of the Supporting Information). While human group I and group II PAKs each share >70% PBD sequence identity, all *E. histolytica* PAK PBD pairs exhibit <70% identity, with the exception of EhPAK2 and EhPAK5 (76% identity). The *E. histolytica* Rho GTPases are similarly diverse, with only four pairs being >70% identical (Figure S1 of the Supporting Information). Although EhPAK4 and EhPAK5 differ substantially, in that EhPAK5 possesses an N-terminal PH domain and the sequences of the kinase domains are only 56% similar

DOI: 10.1021/bi501226f
Biochemistry 2015, 54, 404−412

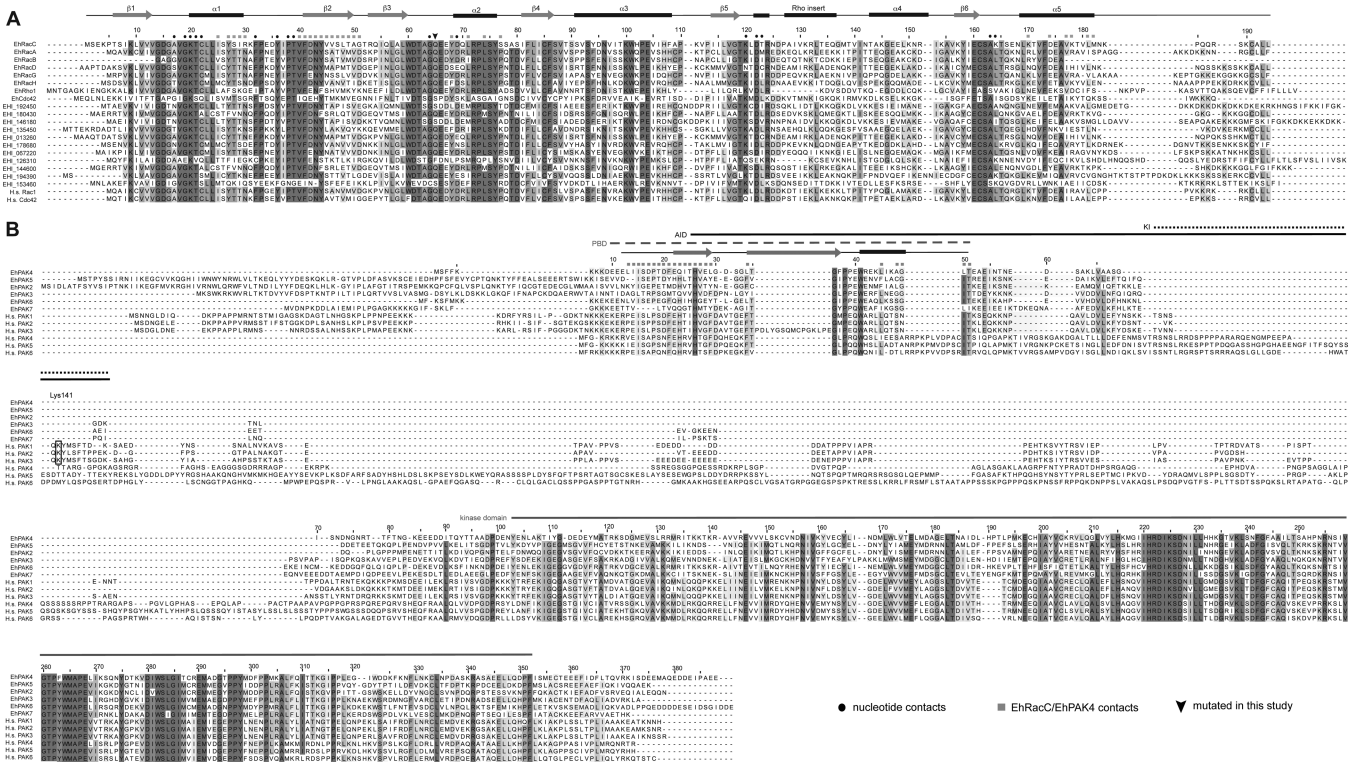

Figure 1. Sequence comparison of *E. histolytica* Rho family GTPases and PAKs. (A) Nineteen *E. histolytica* Rho family GTPases with microarray evidence of transcription[20] are aligned with human homologues. The indicated contacts and secondary structure elements are derived from the crystal structure of the EhRacC^{Q65L}·GTP/EhPAK4 PBD complex presented in this study. EhRacC/EhPAK4 contacts, denoted by gray squares, were defined as coordinates within 1 Å of the binding partner. Increasingly dark shading reflects a higher level of sequence identity. (B) Five putative *E. histolytica* p21-activated kinases (PAKs) are aligned with human group I (PAK1−3) and group II (PAK 4−6) PAKs. The indicated contacts and secondary structure are derived from the crystal structure of the EhRacC^{Q65L}·GTP/EhPAK4 complex, while the p21 binding domain (PBD), autoinhibitory domain (AID), kinase inhibitory segment (KI), and kinase domain all reflect human PAK1.[7] AmoebaDB accession numbers are EHI_152540 for EhPAK4, EHI_148900 for EhPAK2, EHI_148280 for EhPAK3, EHI_043140 for EhPAK5, EHI_186750 for EhPAK6, and EHI_192540 for EhPAK7.

(compared to ∼98% similar among human group I PAK kinase domains), their respective PBDs are more closely related (69% similar), consistent with our observation of both *E. histolytica* PAKs engaging EhRacC.

A Crystal Structure of Activated EhRacC in Complex with the EhPAK4 PBD. A number of functional studies of PAKs in *E. histolytica* have revealed their importance for pathogenesis-related processes;[23−25,35] however, no structural information had yet emerged. We sought to elucidate determinants of Rho/PAK specificity in *E. histolytica* and to compare this GTPase/effector interface with those of well-characterized human homologues. Purified EhRacC^{Q65L}·GTP and EhPAK4 PBD were assembled into a stable 1:1 complex via gel filtration and crystallized. A structural model was obtained from diffraction data extending to 2.35 Å resolution by molecular replacement using human Rac1 as a search model (PDB entry 3TH5). Strong electron density arising from the EhPAK4 PBD (omit map shown in Figure 3) allowed manual building of a structural model. The overall structure of EhRacC is highly similar to that of mammalian Rho family GTPases; a DALI search[36] revealed a 0.6 Å Cα root-mean-square deviation (rmsd) compared to human Rac3 in complex with PAK4 (PDB entry 2OV2). EhRacC also resembles the only other *E. histolytica* Rho family GTPase of known structure, EhRho1 (PDB entry 3REG[20]), with an rmsd of 0.6 Å. In contrast with EhRho1,[20] however, EhRacC possesses the signature "Rho insert" helix (Figure 3A) and retains nucleotide-interacting residues that are highly similar to those of mammalian Rho GTPases (Figure 1A). The EhPAK4 PBD structure consists of a β-hairpin followed by a single α-helix, a motif conserved among the PBDs of human PAKs and WASP.[37,38]

Overall, EhRacC/EhPAK4 interactions bury ∼1150 Å^2 of surface area. The first β-strand of the EhPAK4 PBD extends the six-stranded β-sheet of EhRacC (Figure 3A). In addition to the typical β-sheet backbone interactions, a number of EhPAK4 side chains contribute to a predominantly hydrophobic interface with EhRacC. Leu13 and Ile15 of the EhPAK4 N-terminal extension interact with EhRacC residues Val177 and Leu181 and the hydrophobic portion of Lys178 on helix α5. The EhPAK4 Pro18 residue is universally conserved among PAK PBDs except EhPAK7 (Figure 1B) and occupies a position very similar to that of mammalian PBDs, forming extensive hydrophobic contacts with the aromatic ring of Tyr27 on helix α1 as well as Val46 and Leu48 on strand β2 of EhRacC (Figure 3B). Within the first β-strand of the EhPAK4 PBD, Phe21 makes extensive hydrophobic interactions with EhRacC Tyr47, Ile35, and Ile29. Significant polar interactions also contribute to the EhRacC/EhPAK4 interface in this region. For instance, EhPAK4 residues Gln23 and His26 are within hydrogen bonding distance of EhRacC Asp42. Arg30 in switch 1 of EhRacC likely forms a salt bridge with Asp17 of EhPAK4 (Figure 3B). This contact likely contributes to Rho/effector specificity, because other *E. histolytica* Rho family GTPases lack a basic residue in the position corresponding to Arg30 (Figure

DOI: 10.1021/bi501226f
Biochemistry 2015, 54, 404−412

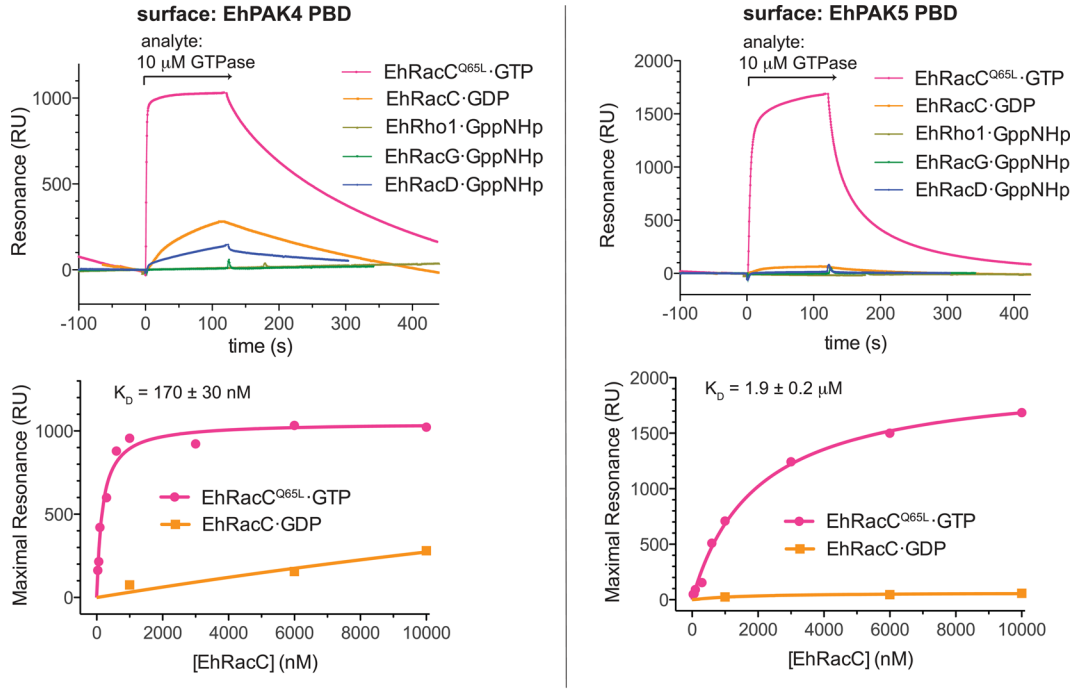

	k_{obs} (s^{-1})	k_{on} (s^{-1} mM^{-1})	k_{off} (s^{-1})	K_D (μM)
EhPAK4	0.0729 ± 0.0021	22.9	0.00409 ± 0.00004	0.178
EhPAK5	0.0389 ± 0.0011	8.46	0.0135 ± 0.0002	1.60

Figure 2. EhPAK4 and EhPAK5 selectively engage activated EhRacC. The isolated PBDs from EhPAK4 and EhPAK5 were immobilized and interactions with four *E. histolytica* Rho family GTPases quantified using surface plasmon resonance (SPR). Rho GTPases were maintained in the activated conformation by being loaded with nonhydrolyzable GTP analogues or, in the case of EhRacC, by mutation of a conserved glutamine (Q65L) required for GTPase activity. Both *E. histolytica* PAKs were found to selectively bind activated EhRacC with high affinity, typical of Rho/effector interactions. Equilibrium binding analyses were performed with active, GTP-bound and inactive, GDP-bound EhRacC. Kinetic parameters of binding were derived from triplicate injections of 3 μM EhRacC. k_{on} was derived from the equation $k_{on} = (k_{obs} - k_{off})/[\text{analyte}]$ and an affinity constant calculated with the equation $K_D = k_{off}/k_{on}$.

1A). Additionally, no other Rho GTPases other than EHI_153460 have a hydrophobic residue in the preceding position (Ile29) and thus likely do not interact optimally with Phe21 of EhPAK4.

The EhPAK4 β-hairpin turn region and the α-helix give rise to a hydrophobic patch that interacts with switch 2 and the C-terminal portion of switch 1 in EhRacC (Figure 3B). Participating residues are Val27, Leu29, Leu34, Leu45, and Ile46 on EhPAK4 and Val40, Phe41, Tyr68, Leu71, and Leu73 on EhRacC. The latter five switch region residues are very well conserved across *E. histolytica* Rho family GTPases (Figure 1A) and, in the case of EhRho1, were seen to make a similar key hydrophobic interface with the GTPase binding domain (GBD) of EhFormin1.[21] Thus, this conserved hydrophobic face may contribute universally to *E. histolytica* Rho/effector interfaces, while specificity is likely dictated by additional interactions.

Structural Diversity of Rho Family GTPase and PBD Interactions. We next sought to compare the EhRacC/EhPAK4 PBD structure with those of similar mammalian Rho/PBD complexes. Structures of human Cdc42 in complex with the PBDs of Wiskott-Aldrich syndrome protein (WASP) (PDB entry 1CEE[37]) or activated Cdc42 kinase (ACK) (PDB entry 1CF4[39]) exhibit a similar interface along strand β2 of Cdc42, as well as contacts at both switch regions (Figure 4). However, the C-terminal portions of the PBDs adopt a structure more extended than that of the EhPAK4 PBD, with ACK lacking clear secondary structure in this region and meandering to the opposite face of switch 2 compared with other Rho/PBD structures. Among the available structures of mammalian Rho family GTPases in complex with PBDs from PAKs, the majority of PAK PBDs adopt a secondary structure, including a β-hairpin and a single α-helix, clearly similar to that of EhRacC/EhPAK4 (Figure 4). Examples shown in Figure 4 include the group I PAK1 PBD in complex with Cdc42 (PDB entry 1E0A[38]) and the group II Cdc42/PAK6 complex (PDB entry 2ODB). However, PAK PBD conformations with a more extended C-terminus lacking the β-hairpin have been observed, as in another NMR structure of Cdc42/PAK1 (PDB entry 1EES[40]), possibly explained by the use of a different PAK PBD peptide. The EhPAK4 PBD differs from each of the mammalian PBDs of known structure in that its C-terminal α-helix lies approximately perpendicular to the β-hairpin strands. In contrast, the α-helices of mammalian PAK PBDs lie approximately parallel to the β-hairpin strands (Figure 4). The ∼90° rotated α-helix of EhPAK4 has a distinct mode of interaction with switch 2 of its Rho GTPase partner. This distinct structural relationship of the β-hairpin and α-helix may be conserved among *E. histolytica* PAKs, as the linkers between these two secondary structure elements are well-conserved, including a dual-proline motif, and switch 2-contacting residues in the α-helix are also well-conserved (Figure 1B). However, the disposition of the EhPAK4 PBD α-helix is likely influenced by an extensive crystal contact interface (buried surface area of

DOI: 10.1021/bi501226f
Biochemistry 2015, 54, 404−412

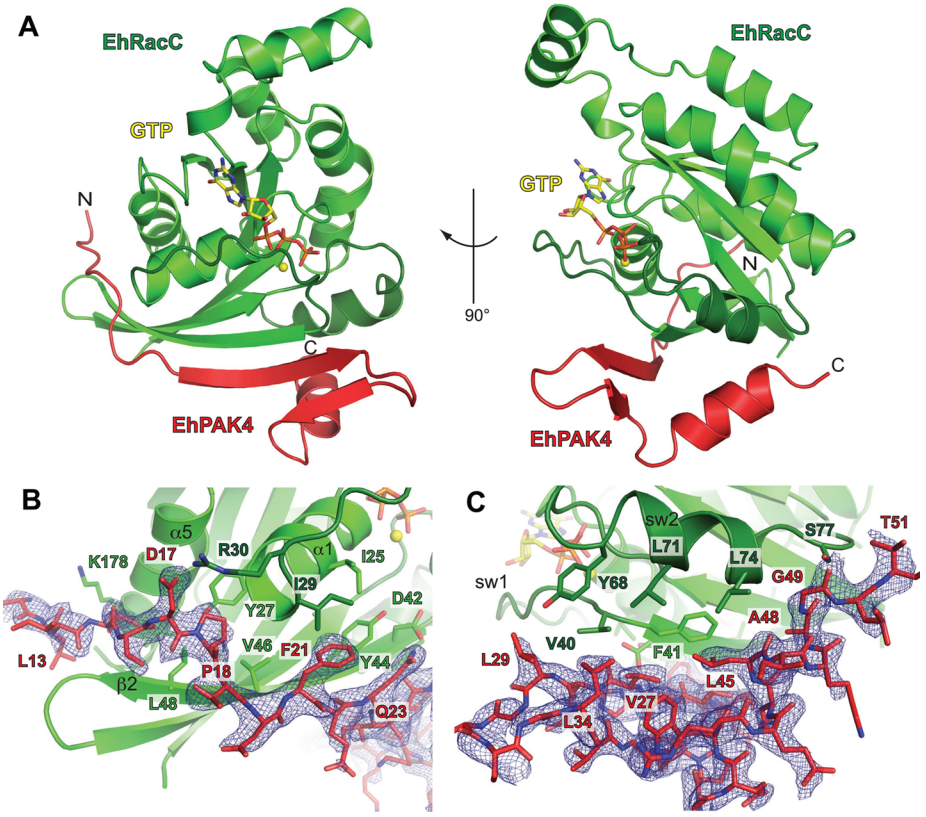

Figure 3. Structural analysis of the interface between EhRacC^{Q65L}·GTP and the PBD of EhPAK4. (A) A complex between EhRacC (green) in its activated conformation and the isolated PBD of EhPAK4 (red) was crystallized and its structure determined to 2.35 Å resolution. The β-sheet central to the typical G domain fold of EhRacC is extended by association with a β-hairpin in the EhPAK4 PBD. (B and C) The EhRacC/PAK4 interface exhibits typical β-sheet backbone interactions, as well as hydrophobic interfaces involving the EhRacC α1, α5, and switch 2 (sw2) helices, switch 1 (sw1), and strand β2. Key polar interactions also likely contribute to binding affinity, e.g., a salt bridge between EhRacC Arg30 and EhPAK4 Asp17. The electron density represents a simulated annealing omit map calculated in the absence of the EhPAK4 model and contoured to 2.5σ.

~9300 Å^2) with an EhRacC/EhPAK4 complex in the neighboring asymmetric unit (Figure 5). The two EhPAK4 α-helices at this interface lie approximately antiparallel to one another, with the tandem basic and acidic residues Arg42 and Glu43 complementing one another (Figure 5). The EhPAK4 α-helices and the two switch 2 regions of the symmetry-related EhRacC molecules also form a hydrophobic interface. Each of the four EhRacC/EhPAK4 complexes in the asymmetric unit makes similar contacts with neighboring dimers. However, there is currently no evidence supporting formation of tetrameric EhRacC/EhPAK4 in solution; e.g., the migration of EhRacC/EhPAK4 upon gel filtration chromatography was consistent with a 1:1 rather than a 2:2 complex. To assess possible effects of the observed crystallographic dimerization on the EhRacC/EhPAK4 complex in solution, we compared the affinity of wild-type EhPAK4 and charge reversal mutant EhPAK4(R42D) for EhRacC·GTP using SPR (Figure 5C). There was no significant difference in affinity with parallel equilibrium binding analyses.

DISCUSSION

Simultaneous expression of ~20 Rho family GTPase genes in the single-cell parasite *E. histolytica* suggests the importance of Rho signaling for trophozoite biology and pathogenesis,[17] as well as likely highly specific signaling to downstream effectors. Studies of Rho GTPase signaling specificity have so far supported this hypothesis. For instance, the diaphanous-related formin EhFormin1 engages EhRho1 to the exclusion of numerous other Rho family GTPases,[21] EhPAK2 interacts with EhRacA but not EhRho1,[23] and the current study reveals EhPAK4 and EhPAK5 are highly selective for EhRacC. A comparison of the EhRacC/EhPAK4 PBD structure with that of EhRho1/EhFormin1[21] revealed a primary hydrophobic interface involving highly conserved residues in the Rho family GTPase switch regions. The specificity of Rho/effector interactions is likely determined by secondary interfaces, such as those involving less well-conserved regions in strand β2 and helices α1 and α5 in EhRacC or helix α3 in EhRho1.[21]

The majority of EhPAK4 PBD residues with side chains contributing to the EhRacC interface are well-conserved in EhPAK5, consistent with shared specificity for a single Rho GTPase. Although the sequences of the PBDs and isolated Rac interface residues are 69 and 62% identical, respectively, the observed differences are not expected to prohibit binding to EhRacC. For instance, Asp17 of EhPAK4 forms a salt bridge with Arg30 of EhRacC (Figure 3B); a glutamate residue of EhPAK5 in the corresponding position likely fulfills a similar function. Phe21 of EhPAK4 (Figure 3B) and a tyrosine of EhPAK5 likewise are probably interchangeable in contributing to a hydrophobic EhRacC interface. The greater affinity of EhRacC for EhPAK4 than for EhPAK5 may be explained by more subtle variation at the Rac/PAK interface. Gln23 of EhPAK4 is within hydrogen bonding distance of Asp42 and Tyr44 of EhRacC (Figure 3B), an interaction that may be less optimally accomplished by a corresponding histidine in EhPAK5. Ala48 of EhPAK4 lies at a hydrophobic interface

DOI: 10.1021/bi501226f
Biochemistry 2015, 54, 404−412

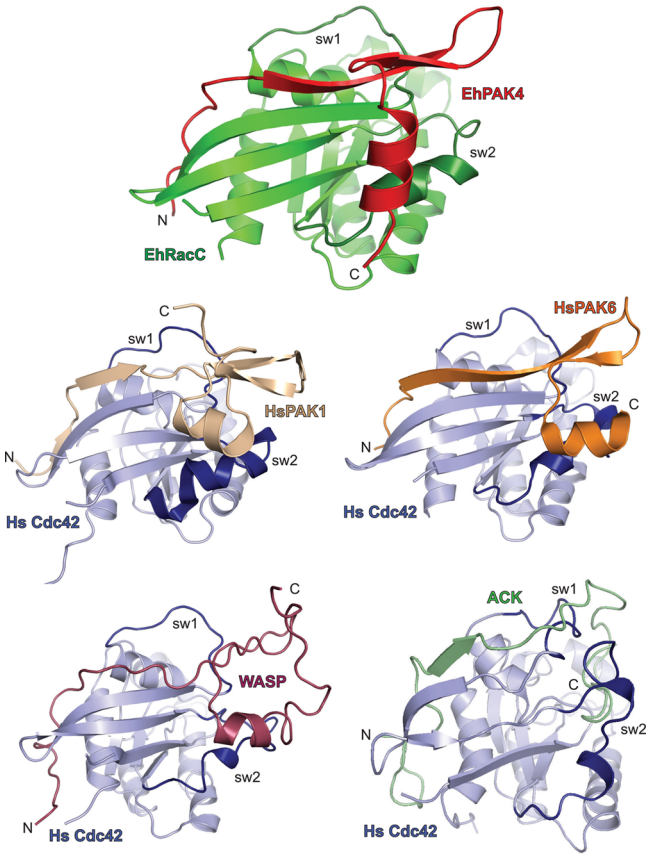

Figure 4. Structural diversity of Rho family GTPase and PBD interactions. The structure of the EhRacC/EhPAK4 PBD complex exhibits similarity to structures of human Cdc42 in complex with multiple PBD-containing effectors (Hs PAK1, PDB entry 1E0A;[38] Hs PAK6, PDB entry 2ODB; Hs WASP, PDB entry 1CEE;[37] Hs ACK, PDB entry 1CF4[39]). The N-terminus of each PBD extends along strand β2 of its GTPase binding partner, often also contacting helix α5 at the C-terminus of each G domain. The C-termini of PBDs are more structurally diverse, with the PAK-derived PBDs typically forming a β-hairpin followed by an α-helix. In contrast, the PBDs of WASP and ACK display more extended C-termini with distinctive Cdc42 interfaces. Although the EhPAK4 PBD is clearly structurally similar to mammalian PAKs, its α-helix adopts a unique orientation, being approximately perpendicular to the β-hairpin strands rather than parallel to them, as seen in mammalian homologues. However, the disposition of the EhPAK4 PBD α-helix may be influenced by crystal contacts (Figure 5).

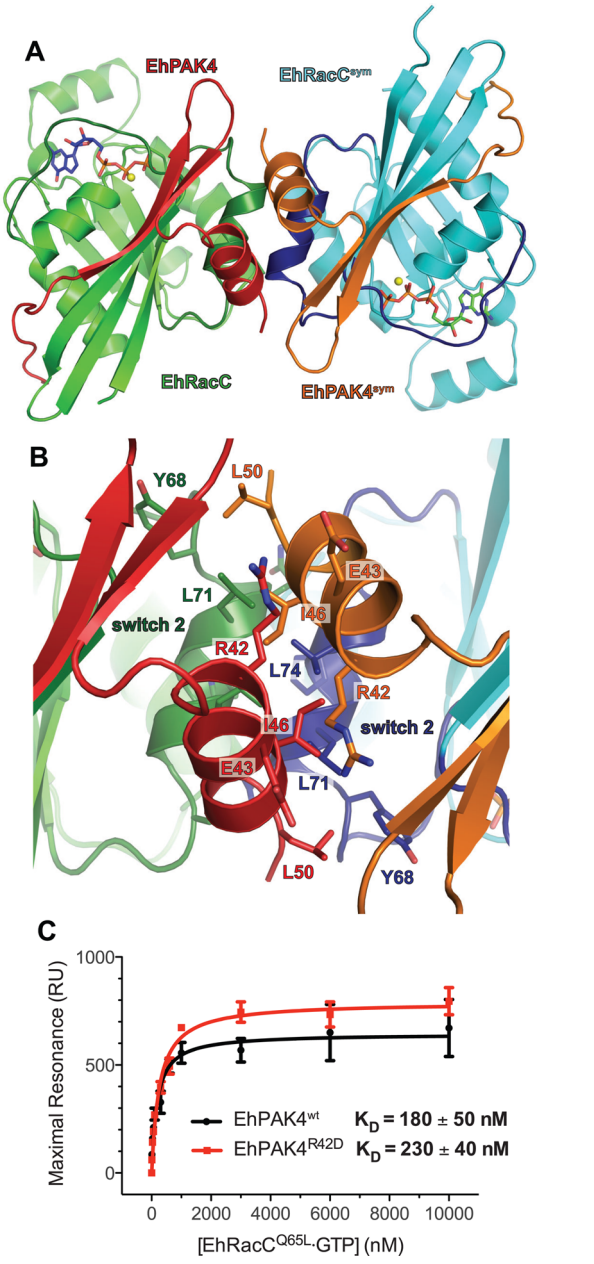

Figure 5. Crystal contacts at the EhPAK4 α-helix and switch 2 of EhRacC. (A) One of four EhRacC/EhPAK4 dimers in the asymmetric unit is shown making contacts with a symmetry-related dimer (EhRacC^{sym}/EhPAK4^{sym}). (B) The α-helices of the PBDs lie in an antiparallel orientation and make complementary ionic interactions through residues Arg42 and Glu43. A hydrophobic interface between symmetry-related dimers arises primarily between switches 2 of EhRacC and the α-helices of EhPAK4 PBD, burying ~9500 Å^2 of surface area. Each of the four EhRacC/EhPAK4 dimers in the asymmetric unit shares a similar interface with a symmetry-related dimer. (C) Charge reversal at the crystal contact site (EhPAK^{R42D}) does not significantly alter the affinity for EhRacC·GTP as measured by SPR. Equilibrium binding affinity constants are reported with the standard error of the mean.

with EhRacC (Figure 3C), and the crystal structure model would not accommodate the larger corresponding EhPAK5 cysteine residue, suggesting structural differences in this peripheral aspect of the Rac/PAK interface.

Despite a high degree of selectivity among studied *E. histolytica* effectors for their Rho GTPase partners, EhRacC has emerged as being capable of engaging a plurality of effectors. In addition to EhPAK4 and EhPAK5, activated EhRacC directly engages the heterotrimeric G protein effector EhRGS-RhoGEF and cooperates with EhGα1 to promote downstream Rac activation.[22] EhRacC may serve as a node for multiple downstream signaling pathways in *E. histolytica*.

Three previously described PAKs in *E. histolytica* have been implicated in major pathogenesis-related cellular processes, including amoebic migration, polarity, phagocytosis, and collagen matrix invasion.[23,24] Further experimentation is needed to assess biological functions of the EhRacC effectors EhPAK4 and EhPAK5. These Rho family GTPase signaling pathways may provide feasible targets for pharmacological manipulation, given previous success with mammalian PAK inhibitors.[12,41] Specific targeting of *E. histolytica* PAKs,

DOI: 10.1021/bi501226f
Biochemistry 2015, 54, 404−412

particularly at the Rho GTPase/PBD interface, is potentially a viable means of perturbing pathogenesis of this serious waterborne intestinal parasite.

■ ASSOCIATED CONTENT

Supporting Information

Tables of sequence identities for *E. histolytica* Rho GTPases and p21-activated kinases. This material is available free of charge via the Internet at http://pubs.acs.org.

■ AUTHOR INFORMATION

Corresponding Author

*Address: 3051A Health Sciences North, P.O. Box 9229, West Virginia University School of Medicine, Morgantown, WV 26506-9229. E-mail: dpsiderovski@hsc.wvu.edu. Telephone: (304) 293-4991.

Funding

Work in the Siderovski lab was supported by National Institutes of Health Grant GM082892, and D.E.B. was supported by an individual NRSA predoctoral fellowship from the National Institute of Diabetes and Digestive and Kidney Diseases (F30DK091978).

Notes

The authors declare no competing financial interest.

■ ACKNOWLEDGMENTS

We thank Drs. Michael Miley and Mischa Machius at the University of North Carolina (UNC) Center for Structural Biology for crystallographic assistance and Biacore 3000 access and Ashutosh Tripathy at the UNC Macromolecular Interactions Facility for ProteOn XPR36 access. We also thank Dr. Channing Der and Nicole Baker for helpful conversations. Crystallographic experiments were conducted at the 23-ID-B beamline at the Advanced Photon Source (Argonne National Laboratory).

■ ABBREVIATIONS

ACK, activated Cdc42 kinase; AID, autoinhibitory domain; IPTG, isopropyl β-D-thiogalactopyranoside; KI, kinase inhibitory domain; NTA, nickel-nitrilotriacetic acid; PAK, p21-activated kinase; PBD, p21 binding domain; RU, resonance unit; SPR, surface plasmon resonance; TEV, tobacco etch virus; WASP, Wiskott-Aldrich syndrome protein.

■ REFERENCES

(1) Hall, A., and Nobes, C. D. (2000) Rho GTPases: Molecular switches that control the organization and dynamics of the actin cytoskeleton. *Philos. Trans. R. Soc. London 355*, 965−970.

(2) Wennerberg, K., and Der, C. J. (2004) Rho-family GTPases: It's not only Rac and Rho (and I like it). *J. Cell Sci. 117*, 1301−1312.

(3) Worthylake, D. K., Rossman, K. L., and Sondek, J. (2000) Crystal structure of Rac1 in complex with the guanine nucleotide exchange region of Tiam1. *Nature 408*, 682−688.

(4) Vigil, D., Cherfils, J., Rossman, K. L., and Der, C. J. (2010) Ras superfamily GEFs and GAPs: Validated and tractable targets for cancer therapy? *Nat. Rev. Cancer 10*, 842−857.

(5) Arias-Romero, L. E., and Chernoff, J. (2008) A tale of two Paks. *Biol. Cell 100*, 97−108.

(6) Baskaran, Y., Ng, Y. W., Selamat, W., Ling, F. T., and Manser, E. (2012) Group I and II mammalian PAKs have different modes of activation by Cdc42. *EMBO Rep. 13*, 653−659.

(7) Lei, M., Lu, W., Meng, W., Parrini, M. C., Eck, M. J., Mayer, B. J., and Harrison, S. C. (2000) Structure of PAK1 in an autoinhibited conformation reveals a multistage activation switch. *Cell 102*, 387−397.

(8) Zhu, G., Wang, Y., Huang, B., Liang, J., Ding, Y., Xu, A., and Wu, W. (2012) A Rac1/PAK1 cascade controls β-catenin activation in colon cancer cells. *Oncogene 31*, 1001−1012.

(9) Eblen, S. T., Slack, J. K., Weber, M. J., and Catling, A. D. (2002) Rac-PAK signaling stimulates extracellular signal-regulated kinase (ERK) activation by regulating formation of MEK1-ERK complexes. *Mol. Cell. Biol. 22*, 6023−6033.

(10) Kichina, J. V., Goc, A., Al-Husein, B., Somanath, P. R., and Kandel, E. S. (2010) PAK1 as a therapeutic target. *Expert Opin. Ther. Targets 14*, 703−725.

(11) Ong, C. C., Jubb, A. M., Zhou, W., Haverty, P. M., Harris, A. L., Belvin, M., Friedman, L. S., Koeppen, H., and Hoeflich, K. P. (2011) p21-activated kinase 1: PAK'ed with potential. *Oncotarget 2*, 491−496.

(12) Deacon, S. W., Beeser, A., Fukui, J. A., Rennefahrt, U. E., Myers, C., Chernoff, J., and Peterson, J. R. (2008) An isoform-selective, small-molecule inhibitor targets the autoregulatory mechanism of p21-activated kinase. *Chem. Biol. 15*, 322−331.

(13) Viaud, J., and Peterson, J. R. (2009) An allosteric kinase inhibitor binds the p21-activated kinase autoregulatory domain covalently. *Mol. Cancer Ther. 8*, 2559−2565.

(14) Haque, R., Huston, C. D., Hughes, M., Houpt, E., and Petri, W. A., Jr. (2003) Amebiasis. *N. Engl. J. Med. 348*, 1565−1573.

(15) Ravdin, J. I. (2000) *Amoebiasis*, Imperial College Press, London.

(16) Meza, I., Talamas-Rohana, P., and Vargas, M. A. (2006) The cytoskeleton of *Entamoeba histolytica*: Structure, function, and regulation by signaling pathways. *Arch. Med. Res. 37*, 234−243.

(17) Bosch, D. E., and Siderovski, D. P. (2013) G protein signaling in the parasite *Entamoeba histolytica*. *Exp. Mol. Med. 45*, e15.

(18) Guillen, N., Boquet, P., and Sansonetti, P. (1998) The small GTP-binding protein RacG regulates uroid formation in the protozoan parasite *Entamoeba histolytica*. *J. Cell Sci. 111* (Part 12), 1729−1739.

(19) Ghosh, S. K., and Samuelson, J. (1997) Involvement of p21racA, phosphoinositide 3-kinase, and vacuolar ATPase in phagocytosis of bacteria and erythrocytes by *Entamoeba histolytica*: Suggestive evidence for coincidental evolution of amebic invasiveness. *Infect. Immun. 65*, 4243−4249.

(20) Bosch, D. E., Wittchen, E. S., Qiu, C., Burridge, K., and Siderovski, D. P. (2011) Unique structural and nucleotide exchange features of the Rho1 GTPase of *Entamoeba histolytica*. *J. Biol. Chem. 286*, 39236−39246.

(21) Bosch, D. E., Yang, B., and Siderovski, D. P. (2012) *Entamoeba histolytica* Rho1 regulates actin polymerization through a divergent, diaphanous-related formin. *Biochemistry 51*, 8791−8801.

(22) Bosch, D. E., Kimple, A. J., Manning, A. J., Muller, R. E., Willard, F. S., Machius, M., Rogers, S. L., and Siderovski, D. P. (2013) Structural Determinants of RGS-RhoGEF Signaling Critical to *Entamoeba histolytica* Pathogenesis. *Structure 21*, 65−75.

(23) Arias-Romero, L. E., de Jesus Almaraz-Barrera, M., Diaz-Valencia, J. D., Rojo-Dominguez, A., Hernandez-Rivas, R., and Vargas, M. (2006) EhPAK2, a novel p21-activated kinase, is required for collagen invasion and capping in *Entamoeba histolytica*. *Mol. Biochem. Parasitol. 149*, 17−26.

(24) Labruyere, E., Zimmer, C., Galy, V., Olivo-Marin, J.-C., and Guillen, N. (2003) EhPAK, a member of the p21-activated kinase family, is involved in the control of *Entamoeba histolytica* migration and phagocytosis. *J. Cell Sci. 116*, 61−71.

(25) Dutta, S., Sardar, A., Ray, D., and Raha, S. (2007) Molecular and functional characterization of EhPAK3, a p21 activated kinase from *Entamoeba histolytica*. *Gene 402*, 57−67.

(26) Ho, S. N., Hunt, H. D., Horton, R. M., Pullen, J. K., and Pease, L. R. (1989) Site-directed mutagenesis by overlap extension using the polymerase chain reaction. *Gene 77*, 51−59.

(27) Otwinowski, Z., and Minor, W. (1997) Processing of X-ray Diffraction Data Collected in Oscillation Mode. In *Methods in Enzymology*, Academic Press, New York.

(28) Adams, P. D., Afonine, P. V., Bunkoczi, G., Chen, V. B., Davis, I. W., Echols, N., Headd, J. J., Hung, L. W., Kapral, G. J., Grosse-

DOI: 10.1021/bi501226f
Biochemistry 2015, 54, 404−412

Kunstleve, R. W., McCoy, A. J., Moriarty, N. W., Oeffner, R., Read, R. J., Richardson, D. C., Richardson, J. S., Terwilliger, T. C., and Zwart, P. H. (2010) PHENIX: A comprehensive Python-based system for macromolecular structure solution. *Acta Crystallogr. D66*, 213−221.
(29) Emsley, P., Lohkamp, B., Scott, W. G., and Cowtan, K. (2010) Features and development of Coot. *Acta Crystallogr. D66*, 486−501.
(30) Painter, J., and Merritt, E. A. (2006) Optimal description of a protein structure in terms of multiple groups undergoing TLS motion. *Acta Crystallogr. D62*, 439−450.
(31) Kimple, A. J., Muller, R. E., Siderovski, D. P., and Willard, F. S. (2010) A capture coupling method for the covalent immobilization of hexahistidine tagged proteins for surface plasmon resonance. *Methods Mol. Biol. 627*, 91−100.
(32) Kimple, R. J., Willard, F. S., Hains, M. D., Jones, M. B., Nweke, G. K., and Siderovski, D. P. (2004) Guanine nucleotide dissociation inhibitor activity of the triple GoLoco motif protein G18: Alanine-to-aspartate mutation restores function to an inactive second GoLoco motif. *Biochem. J. 378*, 801−808.
(33) Bosch, D. E., Kimple, A. J., Sammond, D. W., Muller, R. E., Miley, M. J., Machius, M., Kuhlman, B., Willard, F. S., and Siderovski, D. P. (2011) Structural determinants of affinity enhancement between GoLoco motifs and G-protein α subunit mutants. *J. Biol. Chem. 286*, 3351−3358.
(34) Bosch, D. E., Kimple, A. J., Muller, R. E., Giguere, P. M., Machius, M., Willard, F. S., Temple, B. R., and Siderovski, D. P. (2012) Heterotrimeric G-protein signaling is critical to pathogenic processes in *Entamoeba histolytica*. *PLoS Pathog. 8*, e1003040.
(35) Labruyere, E., Galy, V., Sansonetti, P., and Guillen, N. (2000) Distribution of a potential p21-activated serine/threonine kinase (PAK) in *Entamoeba histolytica*. *Arch. Med. Res. 31*, S128−S130.
(36) Holm, L., and Rosenstrom, P. (2010) Dali server: Conservation mapping in 3D. *Nucleic Acids Res. 38*, W545−W549.
(37) Abdul-Manan, N., Aghazadeh, B., Liu, G. A., Majumdar, A., Ouerfelli, O., Siminovitch, K. A., and Rosen, M. K. (1999) Structure of Cdc42 in complex with the GTPase-binding domain of the 'Wiskott-Aldrich syndrome' protein. *Nature 399*, 379−383.
(38) Morreale, A., Venkatesan, M., Mott, H. R., Owen, D., Nietlispach, D., Lowe, P. N., and Laue, E. D. (2000) Structure of Cdc42 bound to the GTPase binding domain of PAK. *Nat. Struct. Biol. 7*, 384−388.
(39) Mott, H. R., Owen, D., Nietlispach, D., Lowe, P. N., Manser, E., Lim, L., and Laue, E. D. (1999) Structure of the small G protein Cdc42 bound to the GTPase-binding domain of ACK. *Nature 399*, 384−388.
(40) Gizachew, D., Guo, W., Chohan, K. K., Sutcliffe, M. J., and Oswald, R. E. (2000) Structure of the complex of Cdc42Hs with a peptide derived from P-21 activated kinase. *Biochemistry 39*, 3963−3971.
(41) Zhao, Z. S., and Manser, E. (2010) Do PAKs make good drug targets? *F1000 Biology Reports 2*, 70.

DOI: 10.1021/bi501226f
Biochemistry 2015, 54, 404−412